eprints@whiterose.ac.uk
https://eprints.whiterose.ac.uk/

Power-Law Entanglement Spectrum in Many-Body Localized Phases

Maksym Serbyn[1], Alexios A. Michailidis[2], Dmitry A. Abanin[3], and Z. Papić[4]

[1] *Department of Physics, University of California, Berkeley, California 94720, USA*
[2] *School of Physics and Astronomy, University of Nottingham, Nottingham, NG7 2RD, UK*
[3] *Department of Theoretical Physics, University of Geneva,*
24 quai Ernest-Ansermet, 1211 Geneva, Switzerland and
[4] *School of Physics and Astronomy, University of Leeds, Leeds, LS2 9JT, United Kingdom*
(Dated: September 6, 2016)

Entanglement spectrum of the reduced density matrix contains information beyond the von Neumann entropy and provides unique insights into exotic orders or critical behavior of quantum systems. Here we show that strongly-disordered systems in the many-body localized phase have universal power-law entanglement spectra, arising from the presence of extensively many local integrals of motion. The power-law entanglement spectrum distinguishes many-body localized systems from ergodic systems, as well as from ground states of gapped integrable models or systems in the vicinity of scale-invariant critical points. We confirm our results using large-scale exact diagonalization. In addition, we develop a matrix-product state algorithm which allows us to access the eigenstates of large systems close to the localization transition, and discuss general implications of our results for variational studies of highly excited eigenstates in many-body localized systems.

Introduction.— Recently, much progress has been made towards understanding the mechanisms of ergodicity and its breakdown in an isolated quantum many-body system. Currently, two generic classes of many-body systems are known: ergodic (thermal) systems and many-body localized (MBL) systems [1–4]. An ergodic system is one that acts as a heat bath for its subsystems, and therefore thermalizes as a result of unitary evolution [5–7]. By contrast, in MBL systems transport of energy is quenched by disorder, via a mechanism akin to the single-particle Anderson localization [8]. Nevertheless, MBL systems do reach stationary states [9, 10], which are highly non-thermal due to the emergence of extensively many quasi-local integrals of motion (LIOMs) [11–13].

In addition to distinct dynamical properties, ergodic and MBL systems are sharply distinguished by the microscopic nature of their eigenstates. This difference can be probed via quantum-information measures, such as entanglement entropy (EE). Given a pure quantum state ψ of a many-body system $\mathcal{S} = \mathcal{L} \cup \mathcal{R}$, consisting of two subsystems $\mathcal{L}$ and $\mathcal{R}$, the EE is defined as $S = -\sum_i^D \lambda_i \ln \lambda_i$, where $\{\lambda_i\}$, $i = 1, ..., D$, are the eigenvalues of the reduced density matrix $\hat{\rho}_\mathcal{R} = \text{Tr}_\mathcal{L} |\psi\rangle\langle\psi|$, and D is the dimensionality of the Hilbert space of $\mathcal{R}$. The EE of highly-excited eigenstates of thermal systems, which obey the "Eigenstate Thermalization Hypothesis" [5–7], is known to generically scale as the number of degrees of freedom in $\mathcal{R}$ ("volume law"). On the other hand, in an MBL system the EE of nearly all eigenstates obeys the "area law" [11, 12, 14]. This weaker scaling of EE makes MBL systems reminiscent of ground states of gapped systems [15].

EE, while providing a quantitative measure of entanglement in a many-body state, contains no information about how it is created or how different degrees of freedom are entangled with each other. Therefore, to gain

a better understanding of the structure of MBL and ergodic states, we study the "entanglement spectrum" (ES) [16], i.e., the full eigenspectrum of the reduced density matrix, $\{\lambda_i\}$. The ES has been extensively studied in free fermion [17] and critical systems [18]. A particular advantage of the ES is that it can characterize and classify exotic quantum orders that cannot be described by symmetry-breaking [16, 19–21].

In this paper, we obtain a more complete understanding of the eigenstate entanglement properties in the MBL phase and in the vicinity of the delocalization transition. We demonstrate that the ES in the MBL phase has a universal *power-law structure*, whose exponent is proportional to the many-body localization length [Fig. 1]. This structure results from the fact that the ES probes the correlations at the boundary between the subsystems $\mathcal{L}$ and $\mathcal{R}$, and due to the existence of an extensive number of local operators that commute with the Hamiltonian in the MBL phase [11–13]. Thus, the universal power-law distinguishes MBL systems from ergodic systems where the ES obeys the Marchenko-Pastur distribution [22, 23]. Moreover, the power-law spectrum reveals a difference between MBL systems and ground states of gapped integrable models [24] or free systems in the vicinity of scale-invariant critical points [18, 25], where the ES typically decays faster than power law [17, 18, 26, 27].

In addition to providing new insights into the properties of MBL systems, the ES is of crucial importance for the matrix-product state (MPS) optimization algorithms such as the "density matrix renormalization group" (DMRG) [28]. While in principle the MPS naturally encode the eigenstates of MBL phase due to the area-law entropy, practical realizations of the efficient optimization algorithms are an active area of research [29–33]. In this work we develop an MPS optimization to tar-
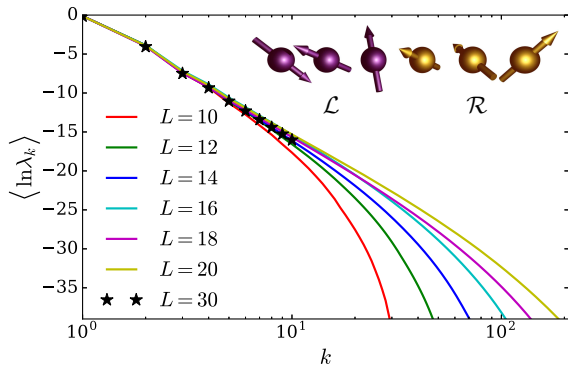
Figure 1. (Color online) ES of the highly-excited eigenstates of XXZ spin chain with disorder strength $W = 5$. The spectrum has a power law form in the MBL phase and in the vicinity of the delocalization transition.

get the highly-excited states of a disordered XXZ chain in 1D, and use the power-law ES as a sensitive benchmark of its accuracy in large systems up to $L = 30$ spins. Our analytic results for the ES allow us to put bounds on the bond dimension, and demonstrate the feasibility of the DMRG calculation of highly excited states in close proximity to the delocalization transition.

Our work complements the recent work by Yang *et al.* [23] and Geraedts *et al.* [34], who studied the ES distribution and level statistics in ergodic and MBL phases, and Monthus [35], who derived the scaling of Renyi entropies in the MBL phase in first-order perturbation in the coupling between the subsystems.

Model.—We consider a standard model of MBL – a XXZ spin-1/2 chain of L spins with a random $z-$field [4]:

$$H = \frac{1}{2} \sum_{i=1}^{L-1} \left[J_x(\sigma_i^x \sigma_{i+1}^x + \sigma_i^y \sigma_{i+1}^y) + J_z \sigma_i^z \sigma_{i+1}^z \right] + \sum_{i=1}^{L} h_i \sigma_i^z, \tag{1}$$

where $h_i \in [-W; W]$ are independent, uniform random numbers, and σ^α are the Pauli matrices. We choose open boundary conditions and assume a bipartition that separates the system into equal $\mathcal{L}$ and $\mathcal{R}$ parts [Fig 1, inset].

The model (1) has been extensively studied and is believed to capture all essential properties of the MBL phase and the localization transition. For example, it is known that the model supports an MBL phase at strong disorder, an ergodic phase at weaker disorder, and an integrable point at zero disorder. For $J_x = J_z = 1$, the transition between the two phases was estimated to be at $W_c \approx 3.5$ based on a variety of probes, for example the level statistics [4, 36, 37], fluctuations of EE [38], and the statistics of the matrix elements of local operators [39].

Power-law entanglement spectrum.— Before discussing numerical results for the model (1), we infer the general properties of the ES in the MBL phase from the existence of LIOMs [11–13, 40]. In the "fully" MBL phase (i.e.,

when there is no mobility edge in the spectrum [36, 39]), there exists a quasi-local unitary transformation which diagonalizes the Hamiltonian by rotating the physical spins σ_i into the exactly conserved LIOMs τ_i. The latter form a complete basis of the Hilbert space, and any many-body eigenstate is a simultaneous eigenstate of all τ_i^z, $i = 1, \ldots L$.

Let us expand a given eigenstate $|I\rangle$ over the complete basis formed by tensor product of eigenstates in $\mathcal{L}$ and $\mathcal{R}$:

$$|I\rangle = \sum_{\{\mu\}_{\mathcal{L}}, \{\tau\}_{\mathcal{R}}} C_{\{\mu\}_{\mathcal{L}}\{\tau\}_{\mathcal{R}}} |\{\mu\}_{\mathcal{L}}\rangle \otimes |\{\tau\}_{\mathcal{R}}\rangle. \tag{2}$$

In the MBL phase, the values of LIOMs in $\mathcal{L}$ or $\mathcal{R}$, $\{\mu\}_{\mathcal{L}}$ and $\{\tau\}_{\mathcal{R}}$ respectively, label the basis vectors. In this basis, the reduced density matrix of the state (2) for $\mathcal{R}$ subsystem reads $\langle\{\chi\}_{\mathcal{R}}|\hat{\rho}_{\mathcal{R}}|\{\tau\}_{\mathcal{R}}\rangle = \sum_{\{\mu\}_{\mathcal{L}}} C^*_{\{\mu\}_{\mathcal{L}}\{\chi\}_{\mathcal{R}}} C_{\{\mu\}_{\mathcal{L}}\{\tau\}_{\mathcal{R}}}$, where the sum over all configurations of the $\mathcal{L}$ subsystem arises from partial trace. We rewrite this matrix as $\hat{\rho}_{\mathcal{R}} = \sum_{\{\mu\}_{\mathcal{L}}} |\psi_{\{\mu\}_{\mathcal{L}}}\rangle\langle\psi_{\{\mu\}_{\mathcal{L}}}|$. The vectors $|\psi_{\{\mu\}_{\mathcal{L}}}\rangle$ are given by the coefficients in Eq. (2):

$$|\psi_{\{\mu\}_{\mathcal{L}}}\rangle = \left(C_{\{\mu\}_{\mathcal{L}}\{\tau_1\}_{\mathcal{R}}}, C_{\{\mu\}_{\mathcal{L}}\{\tau_2\}_{\mathcal{R}}} \ldots, C_{\{\mu\}_{\mathcal{L}}\{\tau_{D_{\mathcal{R}}}\}_{\mathcal{R}}} \right)^T, \tag{3}$$

where each of $D_{\mathcal{R}} = 2^{L_{\mathcal{R}}}$ components is labeled by the different configurations of LIOMs in $\mathcal{R}$.

Deep in the MBL phase, to the order $\mathcal{O}(1)$, an eigenstate $|I\rangle$ of the full system is a product state of certain eigenstates of $\mathcal{L}$ and $\mathcal{R}$ subsystems. Let us define the LIOMs such that these eigenstates are labelled by configurations with all effective spins pointing up, $\tau_i^z|I\rangle = |I\rangle$ for all i. Then, in the expansion (2), the largest coefficient is $|C_{\{\mu\}_{\mathcal{L}}\{\tau\}_{\mathcal{R}}}| = c_0$, with both $\{\tau\}_{\mathcal{R}}$ and $\{\mu\}_{\mathcal{L}} = \uparrow\uparrow \ldots \uparrow$. The typical value of a coefficient with some of the LIOMs flipped is suppressed as

$$|C_{\{\uparrow\ldots\uparrow\underbrace{\downarrow\downarrow\uparrow\}_{\mathcal{L}}}_{r}\{\uparrow\uparrow\downarrow\uparrow\ldots\uparrow\}_{\mathcal{R}}}| \approx c_0 e^{-\kappa r}, \tag{4}$$

where r specifies the "radius of the disturbance" (RoD) of effective spins near the entanglement cut, and κ is the inverse characteristic (many-body) localization length. Note that κ may fluctuate depending on disorder pattern, and should not be taken as a direct analogue of the single-particle localization length as it does not diverge at the transition [39].

If we order the basis in $\mathcal{R}$ according to the RoD, the exponential suppression (4) implies that (i) all terms in $|\psi_{\{\mu\}_{\mathcal{L}}}\rangle$ are suppressed as $e^{-\kappa r_{\mathcal{L}}}$, where $r_{\mathcal{L}}$ is the RoD in the left subsystem; (ii) components of $|\psi_{\{\mu\}_{\mathcal{L}}}\rangle$ are ordered according to their magnitude, so that the first term (corresponding to no spin flips in $\mathcal{R}$) is of order one, the term with one spin flip is of the order $e^{-\kappa}$, etc. Denoting

$a = e^{-\kappa}$, a typical $|\psi_{\{\mu\}_{\mathcal{L}}}\rangle$ is:

$$|\psi_{\{\mu\}_{\mathcal{L}}}\rangle = a^{r_{\mathcal{L}}}(\alpha_1; \ \alpha_2 a; \ \alpha_3 a^2, \alpha_4 a^2; \ \alpha_5 a^3, \ldots, \alpha_8 a^3;$$
$$\ldots; \ \alpha_{1+D_{\mathcal{R}}/2} a^{L_{\mathcal{R}}}, \ldots, \alpha_{D_{\mathcal{R}}} a^{L_{\mathcal{R}}})^T, \quad (5)$$

where all $|\alpha_i|$ are assumed to be of order one, and we separated the blocks corresponding to the value of RoD $r_{\mathcal{R}} = 0, 1, 2, \ldots, L_{\mathcal{R}}$ by semicolons.

If different vectors $|\psi_{\{\mu\}_{\mathcal{L}}}\rangle$ in Eq. (3) were mutually orthogonal, their norm $\langle\psi_{\{\mu\}_{\mathcal{L}}}|\psi_{\{\mu\}_{\mathcal{L}}}\rangle \propto e^{-2\kappa r_{\mathcal{L}}}$ would give the eigenvalues of $\hat{\rho}_{\mathcal{R}}$, and hence the ES. In the Supplemental Material [41] we demonstrate it is possible to perturbatively orthogonalize the vectors $|\psi_{\{\mu\}_{\mathcal{L}}}\rangle$ deep in the MBL phase where $e^{-\kappa} \ll 1$. This process results in the eigenvalues labeled by the RoD r:

$$\lambda_k^{(r)} = \lambda_{\underbrace{\uparrow\ldots\uparrow\downarrow\ldots\downarrow}_{r}} \propto e^{-4\kappa r}, \quad (6)$$

where $k = 2^{r-1} + 1, \ldots, 2^r$ labels 2^{r-1} different eigenvalues in the block corresponding to RoD r. An extra factor of 2 in the exponent in Eq. (6) compared to the norm of corresponding $|\psi_{\{\mu\}_{\mathcal{L}}}\rangle$ arises from the fact that all components in $|\psi_{\{\mu\}_{\mathcal{L}}}\rangle$, corresponding to blocks with RoD less than r, are cancelled in the process of orthogonalization [41]. Intuitively, this means that the processes, which contribute to eigenvalues with RoD equal to $r_{\mathcal{L}}$ in the $\mathcal{L}$ subsystem, flip the same number of spins in the $\mathcal{R}$ subsystem.

One can view the RoD r, or equivalently the typical number of spin flips, as an effective "quantum number" underlying the structure of the ES. This is analogous to, e.g., the subsystem's momentum perpendicular to the entanglement cut (which also labels the edge states if a system has topological order); similar structure for the XXZ ground state was pointed in Ref. [44].

The hierarchical structure of the reduced density matrix implies a *power-law* structure of the ES as a function of k. Indeed, expressing r as $r \approx \ln k / \ln 2$, and using Eq. (6), we find the typical value of λ_k

$$\lambda_k \propto \frac{1}{k^{\gamma}}, \qquad \gamma \simeq \frac{4\kappa}{\ln 2}. \quad (7)$$

to decay as a power law with exponent set by κ [45].

In addition, we can also understand the finite-size effects in the ES. The power-law holds until the very last block, for which $r = L_{\mathcal{R}}$. The average value of λ_k for $k \gtrsim 2^{L_{\mathcal{R}}-1}$ will deviate from the simple power-law form (7). Instead, $\log \lambda_k$ will be given by the order statistics of the Gaussian distribution arising from log-normal statistics of the coefficients (4) [39, 46] in the MBL phase, which describes accurately the tail of the ES as we demonstrate in [41].

Numerical results.—To study the ES numerically in the XXZ chain (1), we use: (i) full exact diagonalization
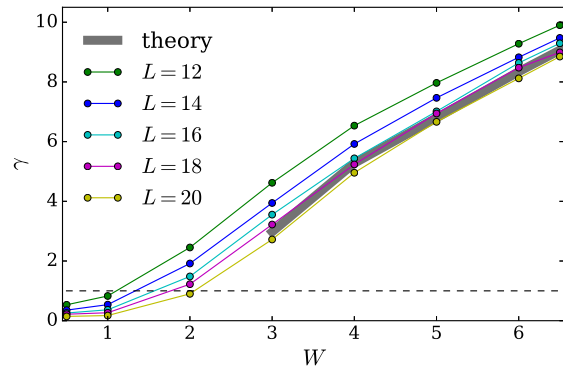

Figure 2. (Color online) Power-law exponent γ, extracted from the fit of the ES, $\langle\ln\lambda_k\rangle$, increases with disorder W. Theoretical prediction refers to γ extracted from the scaling of the matrix elements in Ref. [39].

(ED) for $L = 10, 12, 14$ spins, (ii) "shift and invert" algorithm (SI) [47] for $L = 16, 18, 20$, and (iii) a new implementation of the MPS variational optimization for larger L (below we present data for $L = 30$). Our MPS algorithm combines the advantage of SI spectral transformation, which ensures low energy variance and hence the purity of eigenstates, with a fast conjugate-gradient linear solver. The MPS optimization converges efficiently when the bond dimension χ_{max} is such that $\ln(\chi_{max}) \gg S$, where S is the maximum entropy for all partitions of the chain. Using ITensor libraries [48] with conserved $U(1)$ symmetry and an iterative local scheme, we can reach $\chi_{max} \approx 500$, thus capturing a big part of the ES without finite-bond effects [41].

Fig. 1 illustrates the log-averaged ES, defined as $\{\langle\ln\lambda_k\rangle\}$, where λ_k are ordered from largest to smallest magnitude, and brackets denote averaging over disorder, as a function of the eigenvalue number k, for various system sizes L. Consistent with our expectations (7), in the MBL phase ($W = 5$) the ES exhibits clear power-law behavior. In all cases, we target the eigenstates close to energy $E = 0$, which is roughly in the middle of the many-body band. The data is averaged over a few thousand disorder realizations for $L \leq 16$, and over a few hundred realizations for for $L = 18, 20$. For $L = 30$, we used $\chi_{max} = 200$ and 1000 disorder realizations.

Note that, while we find excellent agreement between ED and MPS results for the few largest Schmidt eigenvalues, the lowest Schmidt values obtained by MPS lie slightly below the ED data for $L = 20$. This is an artefact of our fixed bond dimension $\chi_{max} = 200$, which bounds the slope of the ES through its effect on the smallest Schmidt values. For the given χ_{max}, we expect the MPS slope to be close to the exact slope of the system $L \sim 2\log_2 \chi_{max}$, or $L \sim 14$ in our case (as Fig. 1 confirms). Note that this is a subtle effect which only affects
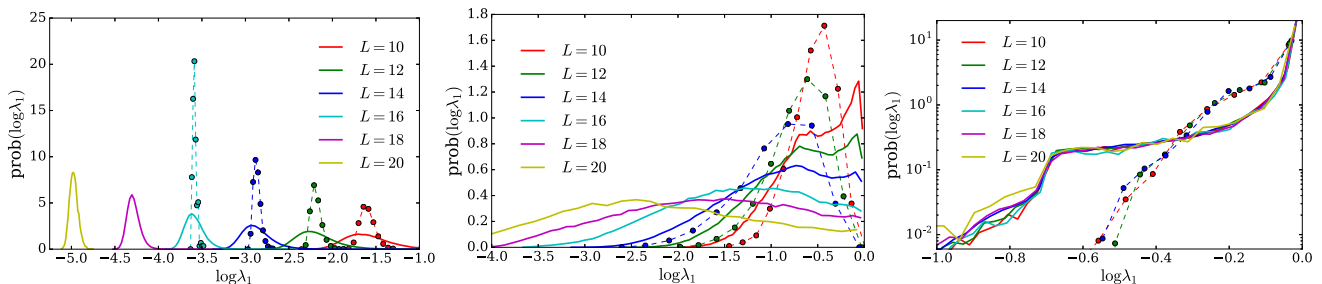
Figure 3. (Color online) Distribution of λ_1 across the MBL transition for different L. Solid lines indicate full distribution, dashed lines show distribution of λ_1 between *different disorder realizations*. Disorder strength is $W = 0.5$ (left), $W = 2$ (middle), $W = 6.5$ (right).

the tail of the ES, while the quantities such as energy or entropy are converged to machine precision [41].

Next, we study the behavior of the exponent γ extracted from the power-law fit of λ_k for small k. The exponent γ always decreases with system size L, as can be seen in Fig. 2. In the MBL phase we expect the exponent to saturate to a finite value, which is set by κ governing the coefficients in Eq. (2). To the leading order in perturbation, the relevant coefficients are a product of matrix elements in $\mathcal{L}$ and $\mathcal{R}$ over the energy denominator Δ, $C_{\{\mu\}_{\mathcal{L}}\{\tau\}_{\mathcal{R}}} \approx \langle\{\mu\}_{\mathcal{L}}|S^{\alpha}_{L/2}|\{\uparrow\}_{\mathcal{L}}\rangle\langle\{\tau\}_{\mathcal{R}}|S^{\alpha}_{L/2+1}|\{\uparrow\}_{\mathcal{R}}\rangle/\Delta$. The typical value of C corresponds to when both matrix elements flip a similar number of spins. The value of κ can be approximated as $\kappa \approx 2\kappa' + \ln 2$, where κ' governs the decay of the many-body analogue of the Thouless conductance $\mathcal{G}$, introduced in Ref. [39]. Fig. 2 shows that this theoretical expectation describes accurately the power-law coefficient γ at sufficiently large L. Note that in the ergodic phase ($W = 0.5$), the power γ is not well defined as the ES obeys a qualitatively different Marchenko-Pastur distribution [23].

Sample-to-sample fluctuations.—So far we discussed behavior of the log-averaged ES. Now we consider the distribution of the ES for different disorder realizations in order to understand whether the ES statistics is dominated by sample-to-sample fluctuations, or rather the fluctuations between different eigenstates in a single disorder realization.

The distribution of the largest ES eigenvalue, λ_1, and its dependence on L is illustrated in Fig. 3. In the ergodic phase ($W = 0.5$), the center of the distribution of λ_1 shifts to smaller values [22], and becomes increasingly narrower with increasing L, reflecting the fact that all eigenstates become typical. On the other hand, deep in the MBL phase, the distribution of λ_1 depends very weakly on L, as expected (Fig. 3, $W = 6.5$). Moreover, the peak in λ_1 is very close to one, indicating that eigenstates in the MBL phase are well-approximated by product states.

Finally, near the transition (Fig. 3, $W = 2$), the distribution of λ_1 becomes very broad, reflecting the fact that

certain disorder realizations are insulating, while others are metallic. Using ED data, we also average the leading eigenvalue over a window of eigenstates from a given disorder realization, and bin the resulting $\langle\log \lambda_1\rangle_{\text{e.s.}}$. Distribution of $\langle\log \lambda_1\rangle_{\text{e.s.}}$, shown by dashed lines in Fig. 3 (middle), has the same width as the full distribution of λ_1. This implies that the broad distribution of λ_1 near the MBL transition originates from sample-to-sample fluctuations, provided that one fixes the position of the entanglement cut. Note, that recently large entanglement fluctuations w.r.t. the position of the cut within the same disorder realization were reported [49].

Discussion.— We demonstrated a power-law decaying ES in MBL states, which is in sharp contrast with both thermal systems, whose ES is "flat" [23], and ground states of gapped free or integrable models, whose ES decays faster than power law [17, 18, 26, 27]. We used this distinct feature of MBL systems to perform highly sensitive benchmarks of our MPS algorithm. Using our algorithm, we obtained eigenstates of large systems at
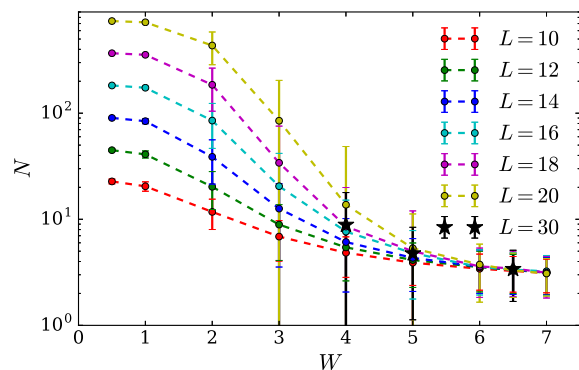

Figure 4. (Color online) Number of singular values required to reproduce the entanglement entropy with fixed precision (99%) decreases with disorder strength W and saturates at strong disorder. The bars represent statistical fluctuations, which are most pronounced near the transition.

disorder $W = 4$, which is closer to the MBL transition than previously reported [29–33].

The power-law ES implies that finite-size effects from the truncation of the ES – a standard procedure in the MPS-like algorithms – typically decay algebraically with L. In Fig. 4 we show the estimate for the MPS bond dimension required to reproduce the exact EE within 1%. While at weak disorder the estimate grows exponentially with L, in the MBL phase it saturates to a constant in a power-law fashion (not shown). Note that even at disorder $W \geq 3$ we have a value of $N \lesssim 100$, hence explaining the success of our MPS algorithm, and suggesting it is feasible to push such algorithms even closer to the MBL transition.

Finally, the organization of the ES according to the number of spin flips by the boundary perturbation may have a number of consequences beyond the power-law structure of ES. In particular, it would be interesting to explore its significance for the ES level statistics studied in Ref. [34], and use it to extract κ and other information about LIOMs from individual eigenstates.

[1] D. Basko, I. Aleiner, and B. Altshuler, *Metal–insulator transition in a weakly interacting many-electron system with localized single-particle states,* Annals of Physics **321**, 1126 – 1205 (2006).

[2] I. V. Gornyi, A. D. Mirlin, and D. G. Polyakov, *Interacting electrons in disordered wires: Anderson localization and low-t transport,* Phys. Rev. Lett. **95**, 206603 (2005).

[3] V. Oganesyan and D. A. Huse, *Localization of interacting fermions at high temperature,* Phys. Rev. B **75**, 155111 (2007).

[4] A. Pal and D. A. Huse, *Many-body localization phase transition,* Phys. Rev. B **82**, 174411 (2010).

[5] J. M. Deutsch, Phys. Rev. A **43**, 2146 (1991).

[6] M. Srednicki, *Chaos and quantum thermalization,* Phys. Rev. E **50**, 888–901 (1994).

[7] M. Rigol, V. Dunjko, and M. Olshanii, *Thermalization and its mechanism for generic isolated quantum systems,* Nature **452**, 854–858 (2008).

[8] P. W. Anderson, *Absence of diffusion in certain random lattices,* Phys. Rev. **109**, 1492–1505 (1958).

[9] M. Serbyn, Z. Papić, and D. A. Abanin, *Quantum quenches in the many-body localized phase,* Phys. Rev. B **90**, 174302 (2014).

[10] M. Serbyn, M. Knap, S. Gopalakrishnan, Z. Papić, N. Y. Yao, C. R. Laumann, D. A. Abanin, M. D. Lukin, and E. A. Demler, *Interferometric probes of many-body localization,* Phys. Rev. Lett. **113**, 147204 (2014).

[11] M. Serbyn, Z. Papić, and D. A. Abanin, *Local conservation laws and the structure of the many-body localized states,* Phys. Rev. Lett. **111**, 127201 (2013).

[12] D. A. Huse, R. Nandkishore, and V. Oganesyan, *Phenomenology of fully many-body-localized systems,* Phys. Rev. B **90**, 174202 (2014).

[13] J. Z. Imbrie, *On many-body localization for quantum spin chains,* Journal of Statistical Physics **163**, 998–1048 (2016).

[14] B. Bauer and C. Nayak, *Area laws in a many-body localized state and its implications for topological order,* Journal of Statistical Mechanics: Theory and Experiment **2013**, P09005 (2013).

[15] M. B. Hastings, *An area law for one-dimensional quantum systems,* Journal of Statistical Mechanics: Theory and Experiment **2007**, P08024 (2007).

[16] H. Li and F. D. M. Haldane, *Entanglement spectrum as a generalization of entanglement entropy: Identification of topological order in non-abelian fractional quantum hall effect states,* Phys. Rev. Lett. **101**, 010504 (2008).

[17] M.-C. Chung and I. Peschel, *Density-matrix spectra of solvable fermionic systems,* Phys. Rev. B **64**, 064412 (2001); I. Peschel and M.-C. Chung, *On the relation between entanglement and subsystem hamiltonians,* EPL (Europhysics Letters) **96**, 50006 (2011).

[18] P. Calabrese and A. Lefevre, *Entanglement spectrum in one-dimensional systems,* Phys. Rev. A **78**, 032329 (2008).

[19] F. Pollmann, A. M. Turner, E. Berg, and M. Oshikawa, *Entanglement spectrum of a topological phase in one dimension,* Phys. Rev. B **81**, 064439 (2010).

[20] L. Fidkowski, *Entanglement spectrum of topological insulators and superconductors,* Phys. Rev. Lett. **104**, 130502 (2010).

[21] H. Yao and X.-L. Qi, *Entanglement entropy and entanglement spectrum of the kitaev model,* Phys. Rev. Lett. **105**, 080501 (2010).

[22] V. A. Marcenko and L. A. Pastur, *Distribution of eigenvalues for some sets of random matrices,* Mathematics of the USSR-Sbornik **1**, 457 (1967).

[23] Z.-C. Yang, C. Chamon, A. Hamma, and E. R. Mucciolo, *Two-component structure in the entanglement spectrum of highly excited states,* Phys. Rev. Lett. **115**, 267206 (2015).

[24] V. Alba, M. Haque, and A. M. Läuchli, *Entanglement spectrum of the heisenberg xxz chain near the ferromagnetic point,* Journal of Statistical Mechanics: Theory and Experiment **2012**, P08011 (2012).

[25] G. Young Cho, A. W. W. Ludwig, and S. Ryu, *Universal Entanglement Spectra of Gapped One-dimensional Field Theories,* ArXiv e-prints (2016), arXiv:1603.04016 [cond-mat.str-el].

[26] K. Okunishi, Y. Hieida, and Y. Akutsu, *Universal asymptotic eigenvalue distribution of density matrices and corner transfer matrices in the thermodynamic limit,* Phys. Rev. E **59**, R6227–R6230 (1999).

[27] F. Franchini, A. R. Its, V. E. Korepin, and L. A. Takhtajan, *Spectrum of the density matrix of a large block of spins of the xy model in one dimension,* Quantum Infor-

mation Processing **10**, 325–341 (2011).

[28] S. R. White, *Density matrix formulation for quantum renormalization groups,* Phys. Rev. Lett. **69**, 2863–2866 (1992).

[29] X. Yu, D. Pekker, and B. K. Clark, *Finding matrix product state representations of highly-excited eigenstates of many-body localized Hamiltonians,* ArXiv e-prints (2015), arXiv:1509.01244 [cond-mat.str-el].

[30] S. P. Lim and D. N. Sheng, *Nature of Many-Body Localization and Transitions by Density Matrix Renormaliztion Group and Exact Diagonalization Studies,* ArXiv e-prints (2015), arXiv:1510.08145 [cond-mat.str-el].

[31] F. Pollmann, V. Khemani, J. I. Cirac, and S. L. Sondhi, *Efficient variational diagonalization of fully many-body localized Hamiltonians,* ArXiv e-prints (2015), arXiv:1506.07179 [cond-mat.str-el].

[32] V. Khemani, F. Pollmann, and S. L. Sondhi, *Obtaining highly-excited eigenstates of many-body localized Hamiltonians by the density matrix renormalization group,* ArXiv e-prints (2015), arXiv:1509.00483 [cond-mat.dis-nn].

[33] D. M. Kennes and C. Karrasch, *Entanglement scaling of excited states in large one-dimensional many-body localized systems,* ArXiv e-prints (2015), arXiv:arXiv:1511.02205 [cond-mat.str-el].

[34] S. D. Geraedts, R. Nandkishore, and N. Regnault, *Many body localization and thermalization: insights from the entanglement spectrum,* ArXiv e-prints (2016), arXiv:1603.00880 [cond-mat.stat-mech].

[35] C. Monthus, *Many-body-localization transition in the strong disorder limit: Entanglement entropy from the statistics of rare extensive resonances,* Entropy **18**, 122 (2016).

[36] D. J. Luitz, N. Laflorencie, and F. Alet, *Many-body localization edge in the random-field heisenberg chain,* Phys. Rev. B **91**, 081103 (2015).

[37] M. Serbyn and J. E. Moore, *Spectral statistics across the many-body localization transition,* Phys. Rev. B **93**, 041424 (2016).

[38] J. A. Kjäll, J. H. Bardarson, and F. Pollmann, *Many-body localization in a disordered quantum ising chain,* Phys. Rev. Lett. **113**, 107204 (2014).

[39] M. Serbyn, Z. Papić, and D. A. Abanin, *Criterion for many-body localization-delocalization phase transition,* Phys. Rev. X **5**, 041047 (2015).

[40] V. Ros, M. Müller, and A. Scardicchio, *Integrals of motion in the many-body localized phase,* Nuclear Physics B **891**, 420 – 465 (2015).

[41] See Supplemental Material, which includes Refs. [42, 43].

[42] J. P. Royston, *Algorithm as 177: Expected normal order statistics (exact and approximate),* Journal of the Royal Statistical Society. Series C (Applied Statistics) **31**, 161–165 (1982).

[43] E. Polak and G. Ribière, *Note sur la convergence de directions conjuguees,* Rev. Francaise Informat Recherche Operationnelle, 3e. Année **16**, 35–43 (1969).

[44] V. Alba, M. Haque, and A. M. Läuchli, *Boundary-locality and perturbative structure of entanglement spectra in gapped systems,* Phys. Rev. Lett. **108**, 227201 (2012).

[45] We note that result (7) is approximate and holds for $\kappa \gg 1$. Our analysis neglects the fact that amplitudes $C_{\{\mu\}_\mathcal{L}\{\tau\}_\mathcal{R}}$ have a broad distribution, with width $\sim 1/2^r$, due to the small energy denominators appearing when these coefficients are calculated perturbatively. In addition, there is some level repulsion due to the fact that off-diagonal matrix elements are of the same order as ES level spacing. Both of these effects will broaden the band corresponding to a block with given RoD. However, this broadening is of the order $2^r e^{-4\kappa r}$ which results only in a small correction to result (7).

[46] A. De Luca and A. Scardicchio, *Ergodicity breaking in a model showing many-body localization,* Europhys. Lett. **101**, 37003 (2013).

[47] V. Hernandez, J. E. Roman, and V. Vidal, *Slepc: A scalable and flexible toolkit for the solution of eigenvalue problems,* ACM Trans. Math. Softw. **31**, 351–362 (2005).

[48] http://itensor.org.

[49] X. Yu, D. J. Luitz, and B. K. Clark, *Bimodal entanglement entropy distribution in the many-body localization transition,* ArXiv e-prints (2016), arXiv:1606.01260 [cond-mat.str-el].